EUROPEAN ORGANISATION FOR NUCLEAR RESEARCH

CERN-EP/2003-010
5 March 2003

Test of non-commutative QED in the process $e^+e^- \to \gamma\gamma$ at LEP

The OPAL Collaboration

Abstract

Non-commutative QED would lead to deviations from the Standard Model depending on a new energy scale $\Lambda_{\rm NC}$ and a unique direction in space defined by two angles η and ξ. Here in this analysis η is defined as the angle between the unique direction and the rotation axis of the earth. The predictions of such a theory for the process $e^+e^- \to \gamma\gamma$ are evaluated for the specific orientation of the OPAL detector and compared to the measurements. Distributions of the polar and azimuthal scattering angles are used to extract limits on the energy scale $\Lambda_{\rm NC}$ depending on the model parameter η. At the 95% confidence level $\Lambda_{\rm NC}$ is found to be larger than 141 GeV for all η and ξ. It is shown that the time dependence of the total cross-section could be used to determine the model parameter ξ if there were a detectable signal. These are the first limits obtained on non-commutative QED from an e^+e^- collider experiment.

To be submitted to Phys. Lett.

The OPAL Collaboration

G. Abbiendi[2], C. Ainsley[5], P.F. Åkesson[3], G. Alexander[22], J. Allison[16], P. Amaral[9], G. Anagnostou[1], K.J. Anderson[9], S. Arcelli[2], S. Asai[23], D. Axen[27], G. Azuelos[18,a], I. Bailey[26], E. Barberio[8,p], R.J. Barlow[16], R.J. Batley[5], P. Bechtle[25], T. Behnke[25], K.W. Bell[20], P.J. Bell[1], G. Bella[22], A. Bellerive[6], G. Benelli[4], S. Bethke[32], O. Biebel[31], I.J. Bloodworth[1], O. Boeriu[10], P. Bock[11], D. Bonacorsi[2], M. Boutemeur[31], S. Braibant[8], L. Brigliadori[2], R.M. Brown[20], K. Buesser[25], H.J. Burckhart[8], S. Campana[4], R.K. Carnegie[6], B. Caron[28], A.A. Carter[13], J.R. Carter[5], C.Y. Chang[17], D.G. Charlton[1,b], A. Csilling[8,g], M. Cuffiani[2], S. Dado[21], A. De Roeck[8], E.A. De Wolf[8,s], K. Desch[25], B. Dienes[30], M. Donkers[6], J. Dubbert[31], E. Duchovni[24], G. Duckeck[31], I.P. Duerdoth[16], E. Elfgren[18], E. Etzion[22], F. Fabbri[2], L. Feld[10], P. Ferrari[8], F. Fiedler[31], I. Fleck[10], M. Ford[5], A. Frey[8], A. Fürtjes[8], P. Gagnon[12], J.W. Gary[4], G. Gaycken[25], C. Geich-Gimbel[3], G. Giacomelli[2], P. Giacomelli[2], M. Giunta[4], J. Goldberg[21], E. Gross[24], J. Grunhaus[22], M. Gruwé[8], P.O. Günther[3], A. Gupta[9], C. Hajdu[29], M. Hamann[25], G.G. Hanson[4], K. Harder[25], A. Harel[21], M. Harin-Dirac[4], M. Hauschild[8], C.M. Hawkes[1], R. Hawkings[8], R.J. Hemingway[6], C. Hensel[25], G. Herten[10], R.D. Heuer[25], J.C. Hill[5], K. Hoffman[9], R.J. Homer[1], D. Horváth[29,c], P. Igo-Kemenes[11], K. Ishii[23], H. Jeremie[18], P. Jovanovic[1], T.R. Junk[6], N. Kanaya[26], J. Kanzaki[23], G. Karapetian[18], D. Karlen[6], K. Kawagoe[23], T. Kawamoto[23], R.K. Keeler[26], R.G. Kellogg[17], B.W. Kennedy[20], D.H. Kim[19], K. Klein[11,t], A. Klier[24], S. Kluth[32], T. Kobayashi[23], M. Kobel[3], S. Komamiya[23], L. Kormos[26], T. Krämer[25], T. Kress[4], P. Krieger[6,l], J. von Krogh[11], K. Kruger[8], T. Kuhl[25], M. Kupper[24], G.D. Lafferty[16], H. Landsman[21], D. Lanske[14], J.G. Layter[4], A. Leins[31], D. Lellouch[24], J. Letts[o], L. Levinson[24], J. Lillich[10], S.L. Lloyd[13], F.K. Loebinger[16], J. Lu[27], J. Ludwig[10], A. Macpherson[28,i], W. Mader[3], S. Marcellini[2], A.J. Martin[13], G. Masetti[2], T. Mashimo[23], P. Mättig[m], W.J. McDonald[28], J. McKenna[27], T.J. McMahon[1], R.A. McPherson[26], F. Meijers[8], W. Menges[25], F.S. Merritt[9], H. Mes[6,a], A. Michelini[2], S. Mihara[23], G. Mikenberg[24], D.J. Miller[15], S. Moed[21], W. Mohr[10], T. Mori[23], A. Mutter[10], K. Nagai[13], I. Nakamura[23], H.A. Neal[33], R. Nisius[32], S.W. O'Neale[1], A. Oh[8], A. Okpara[11], M.J. Oreglia[9], S. Orito[23], C. Pahl[32], G. Pásztor[4,g], J.R. Pater[16], G.N. Patrick[20], J.E. Pilcher[9], J. Pinfold[28], D.E. Plane[8], B. Poli[2], J. Polok[8], O. Pooth[14], M. Przybycień[8,n], A. Quadt[3], K. Rabbertz[8,r], C. Rembser[8], P. Renkel[24], H. Rick[4], J.M. Roney[26], S. Rosati[3], Y. Rozen[21], K. Runge[10], K. Sachs[6], T. Saeki[23], E.K.G. Sarkisyan[8,j], A.D. Schaile[31], O. Schaile[31], P. Scharff-Hansen[8], J. Schieck[32], T. Schörner-Sadenius[8], M. Schröder[8], M. Schumacher[3], C. Schwick[8], W.G. Scott[20], R. Seuster[14,f], T.G. Shears[8,h], B.C. Shen[4], P. Sherwood[15], G. Siroli[2], A. Skuja[17], A.M. Smith[8], R. Sobie[26], S. Söldner-Rembold[16,d], F. Spano[9], A. Stahl[3], K. Stephens[16], D. Strom[19], R. Ströhmer[31], S. Tarem[21], M. Tasevsky[8], R.J. Taylor[15], R. Teuscher[9], M.A. Thomson[5], E. Torrence[19], D. Toya[23], P. Tran[4], A. Tricoli[2], I. Trigger[8], Z. Trócsányi[30,e], E. Tsur[22], M.F. Turner-Watson[1], I. Ueda[23], B. Ujvári[30,e], C.F. Vollmer[31], P. Vannerem[10], R. Vértesi[30], M. Verzocchi[17], H. Voss[8,q], J. Vossebeld[8,h], D. Waller[6], C.P. Ward[5], D.R. Ward[5], P.M. Watkins[1], A.T. Watson[1], N.K. Watson[1], P.S. Wells[8], T. Wengler[8], N. Wermes[3], D. Wetterling[11] G.W. Wilson[16,k], J.A. Wilson[1], G. Wolf[24], T.R. Wyatt[16], S. Yamashita[23], D. Zer-Zion[4], L. Zivkovic[24]

[1]School of Physics and Astronomy, University of Birmingham, Birmingham B15 2TT, UK
[2]Dipartimento di Fisica dell' Università di Bologna and INFN, I-40126 Bologna, Italy
[3]Physikalisches Institut, Universität Bonn, D-53115 Bonn, Germany
[4]Department of Physics, University of California, Riverside CA 92521, USA
[5]Cavendish Laboratory, Cambridge CB3 0HE, UK
[6]Ottawa-Carleton Institute for Physics, Department of Physics, Carleton University, Ottawa, Ontario K1S 5B6, Canada
[8]CERN, European Organisation for Nuclear Research, CH-1211 Geneva 23, Switzerland
[9]Enrico Fermi Institute and Department of Physics, University of Chicago, Chicago IL 60637, USA

[10]Fakultät für Physik, Albert-Ludwigs-Universität Freiburg, D-79104 Freiburg, Germany
[11]Physikalisches Institut, Universität Heidelberg, D-69120 Heidelberg, Germany
[12]Indiana University, Department of Physics, Bloomington IN 47405, USA
[13]Queen Mary and Westfield College, University of London, London E1 4NS, UK
[14]Technische Hochschule Aachen, III Physikalisches Institut, Sommerfeldstrasse 26-28, D-52056 Aachen, Germany
[15]University College London, London WC1E 6BT, UK
[16]Department of Physics, Schuster Laboratory, The University, Manchester M13 9PL, UK
[17]Department of Physics, University of Maryland, College Park, MD 20742, USA
[18]Laboratoire de Physique Nucléaire, Université de Montréal, Montréal, Québec H3C 3J7, Canada
[19]University of Oregon, Department of Physics, Eugene OR 97403, USA
[20]CLRC Rutherford Appleton Laboratory, Chilton, Didcot, Oxfordshire OX11 0QX, UK
[21]Department of Physics, Technion-Israel Institute of Technology, Haifa 32000, Israel
[22]Department of Physics and Astronomy, Tel Aviv University, Tel Aviv 69978, Israel
[23]International Centre for Elementary Particle Physics and Department of Physics, University of Tokyo, Tokyo 113-0033, and Kobe University, Kobe 657-8501, Japan
[24]Particle Physics Department, Weizmann Institute of Science, Rehovot 76100, Israel
[25]Universität Hamburg/DESY, Institut für Experimentalphysik, Notkestrasse 85, D-22607 Hamburg, Germany
[26]University of Victoria, Department of Physics, P O Box 3055, Victoria BC V8W 3P6, Canada
[27]University of British Columbia, Department of Physics, Vancouver BC V6T 1Z1, Canada
[28]University of Alberta, Department of Physics, Edmonton AB T6G 2J1, Canada
[29]Research Institute for Particle and Nuclear Physics, H-1525 Budapest, P O Box 49, Hungary
[30]Institute of Nuclear Research, H-4001 Debrecen, P O Box 51, Hungary
[31]Ludwig-Maximilians-Universität München, Sektion Physik, Am Coulombwall 1, D-85748 Garching, Germany
[32]Max-Planck-Institute für Physik, Föhringer Ring 6, D-80805 München, Germany
[33]Yale University, Department of Physics, New Haven, CT 06520, USA

[a] and at TRIUMF, Vancouver, Canada V6T 2A3
[b] and Royal Society University Research Fellow
[c] and Institute of Nuclear Research, Debrecen, Hungary
[d] and Heisenberg Fellow
[e] and Department of Experimental Physics, Lajos Kossuth University, Debrecen, Hungary
[f] and MPI München
[g] and Research Institute for Particle and Nuclear Physics, Budapest, Hungary
[h] now at University of Liverpool, Dept of Physics, Liverpool L69 3BX, U.K.
[i] and CERN, EP Div, 1211 Geneva 23
[j] now at University of Nijmegen, HEFIN, NL-6525 ED Nijmegen,The Netherlands, on NWO/NATO Fellowship B 64-29
[k] now at University of Kansas, Dept of Physics and Astronomy, Lawrence, KS 66045, U.S.A.
[l] now at University of Toronto, Dept of Physics, Toronto, Canada
[m] current address Bergische Universität, Wuppertal, Germany
[n] and University of Mining and Metallurgy, Cracow, Poland
[o] now at University of California, San Diego, U.S.A.
[p] now at Physics Dept Southern Methodist University, Dallas, TX 75275, U.S.A.
[q] now at IPHE Université de Lausanne, CH-1015 Lausanne, Switzerland
[r] now at IEKP Universität Karlsruhe, Germany
[s] now at Universitaire Instelling Antwerpen, Physics Department, B-2610 Antwerpen, Belgium
[t] now at RWTH Aachen, Germany

1 Introduction

Recently, there has been increasing interest in theories with non-commutative space-time geometries. The idea of non-commutative geometry is not new. It was studied in the 1940s as a possible means of regularising divergences in quantum field theory [1]. More recent interest is related to the possibility that non-commutative geometry may arise in string theory through the quantisation of strings in the presence of background fields [2].

In a quantum field theory of non-commutative geometry the space-time coordinates are represented by operators X_μ satisfying the relation:

$$[X_\mu, X_\nu] = i\theta_{\mu\nu} \tag{1}$$

where $\theta_{\mu\nu}$ is a constant antisymmetric matrix, having units of (length)^2 = (mass)$^{-2}$ $\sim 1/\Lambda^2_{\rm NC}$. This introduces a fundamental scale, $\Lambda_{\rm NC}$, representing the space-time distance below which the space-time coordinates become fuzzy. Its role can be compared to that of the Planck constant h in ordinary quantum mechanics, which quantifies the level of non-commutativity between coordinates and momenta.l Although there is no *a priori* prediction for the scale $\Lambda_{\rm NC}$, it might be at the level of the Planck scale [3, 4]. However, in light of recent progress in string theory and theories with large extra dimensions the energy scale at which gravity becomes strong could be of $\mathcal{O}$(TeV). It is therefore conceivable that $\Lambda_{\rm NC}$ could also be at the TeV scale and that the effects of a non-commutative geometry might be observable in present or planned collider experiments.

The matrix $\theta_{\mu\nu}$ can be decomposed into two independent parts [5, 6]: electric-like components $\boldsymbol{\theta}_E = (\theta_{01}, \theta_{02}, \theta_{03})$ and magnetic-like components $\boldsymbol{\theta}_B = (\theta_{23}, \theta_{31}, \theta_{12})$. The matrix $\theta_{\mu\nu}$ is constant and frame independent, which leads to violation of Lorentz invariance; $\boldsymbol{\theta}_E$ and $\boldsymbol{\theta}_B$ can be considered as 3-vectors which define two unique directions in space.

A non-commutative Standard Model has not yet been formulated. Only QED with non-commutative geometry (NCQED) exists [7]. This theory is known to be invariant under U(1) gauge transformations and renormalisable at the one-loop level. However, there are some limitations in the existing NCQED, for example only charges 0 or ± 1 are allowed and consequently quarks are not incorporated in the theory. Despite these limitations NCQED can be regarded as a consistent theory, and may serve as a test bed for the study of other non-commutative quantum field theories. There are a number of studies of general NCQED phenomenology [3] and specifically at high energy linear colliders [5, 8]. Limits have been obtained at low energy using the Lamb shift [9], the Aharonov-Bohm effect [10] and clock comparisons [11] under specific assumptions. This paper presents the first limits on NCQED obtained from a collider experiment.

In NCQED each eeγ vertex involves a kinematic phase factor $e^{\frac{i}{2}p_1^\mu \theta_{\mu\nu} p_2^\nu}$, where p_1^μ, p_2^ν are the electron momenta. In addition there are non-Abelian-like 3γ and 4γ self couplings, which are proportional to the kinematic phase. The amplitude of a scattering process therefore depends not only on the kinematics of the initial and final state particles, but also on the unique directions $\boldsymbol{\theta}_E$ and $\boldsymbol{\theta}_B$ relative to the orientation of the experiment. The characteristic properties of NCQED may thus be observed as direction-dependent deviations from the predictions of QED. If observed, the unique directions could be inferred. This can be regarded as an analogue of the Michelson-Morley experiment.

In this paper, a purely electromagnetic process $e^+e^- \to \gamma\gamma$ is studied using the high-energy e^+e^- collision data collected with the OPAL detector at LEP. The theoretical calculation corresponds to tree level ($e^+e^- \to \gamma\gamma$). The experimental selection includes higher orders ($e^+e^- \to \gamma\gamma(\gamma)$) and the measured cross-sections are corrected to tree level assuming ordinary QED. Possible higher-order

effects from NCQED are expected to be smaller than effects of fourth order QED and weak interactions which are taken into account by a 1% systematic uncertainty on the cross-section.

2 $e^+e^- \to \gamma\gamma$ in NCQED

In NCQED three diagrams contribute to the process $e^+e^- \to \gamma\gamma$ at the tree level. Two are similar to the ordinary pair-annihilation diagrams of QED, but with a kinematic phase at each vertex. The third diagram is an s-channel photon exchange with $\gamma\gamma\gamma$ self coupling. The differential cross-section for $e^+e^- \to \gamma\gamma$ in NCQED is given by [6]

$$\frac{d^2\sigma}{d\cos\theta d\phi} = \frac{\alpha^2}{s}\frac{1+\cos^2\theta}{1-\cos^2\theta}[1-\sin^2\theta\cdot\sin^2\Delta_{NC}], \tag{2}$$

where θ and ϕ are the polar and azimuthal angles (with respect to the outgoing electron beam) of the final state photon with $0 \le \cos\theta \le 1$, α is the fine-structure constant and s is the centre-of-mass energy squared. This is similar to the QED expression but with a correction arising from NCQED represented by the term in square brackets. The parameter Δ_{NC} is given by

$$\Delta_{NC} = -\frac{s}{4\Lambda_{NC}^2}(c_{01}\sin\theta\cos\phi + c_{02}\sin\theta\sin\phi + c_{03}\cos\theta). \tag{3}$$

Here we have introduced new dimensionless parameters, c_{0i}, defined by

$$\boldsymbol{\theta}_E = \frac{1}{\Lambda_{NC}^2}\mathbf{c}_E = \frac{1}{\Lambda_{NC}^2}(c_{01}, c_{02}, c_{03}) \tag{4}$$

where $\Lambda_{NC} = 1/\sqrt{|\boldsymbol{\theta}_E|}$ and c_{0i} are components of the unit vector $\mathbf{c}_E$ pointing to the unique direction in the coordinate system of the experiment. At tree level the process $e^+e^- \to \gamma\gamma$ is sensitive only to $\boldsymbol{\theta}_E$, not to $\boldsymbol{\theta}_B$. For final state photons which are not back-to-back small effects from the magnetic-like components $\boldsymbol{\theta}_B$ could occur which are neglected in this analysis. Note also that the effect of NCQED on the cross-section for this process is always negative with respect to QED and that the relative size of the effect is larger at large production angles due to the $\sin^2\theta$ term. In general Δ_{NC} depends not just on the photon production angle θ, but also on the azimuthal angle ϕ. This is a signature of the anisotropy of space-time which is inherent in non-commutative geometry. Only in the special case where $\boldsymbol{\theta}_E$ is parallel to the beam electrons ($c_{01} = c_{02} = 0$) does this ϕ dependence vanish. Even in the presence of transverse beam polarisation the QED cross-section is independent of ϕ [12].

The unique direction $\mathbf{c}_E$ is not known. However, if it exists, it is unlikely that it is fixed to the solar system or to the earth. Rather it would be natural to assume that this direction is fixed to some larger structure in space, e.g. the rest frame of the cosmic microwave background. We refer to this as the primary frame. In the coordinate system of an experiment on the earth, the unique direction will change as the earth rotates and as the orientation of the earth's rotation axis changes due to the movement of the galaxy or the solar system with respect to the primary frame. We assume that the latter movement is sufficiently slow that over the timescale of the experiment the rotation of the earth is the only relevant motion. This in turn provides an opportunity to examine the time-dependent effect of NCQED. In the next Section, we consider how the direction c_{0i} varies as a function of the earth's rotation and how Δ_{NC} follows its variation.

3 Vector $\boldsymbol{\theta_E}$ in the experimental laboratory system

The conventions for the primary (X, Y, Z) and local (x, y, z) coordinate systems are shown in Figure 1. We use right-handed Cartesian coordinate systems throughout this paper. For convenience, we choose the axis of the earth's rotation to be the Z-axis of the primary coordinate system. The X-axis points in some fixed direction which can be chosen arbitrarily. The unit vector $\mathbf{c}_E^0$ in the primary frame is specified by two parameters, the polar angle η and the azimuthal angle ξ:

$$\mathbf{c}_E^0 = \begin{pmatrix} s_\eta c_\xi \\ s_\eta s_\xi \\ c_\eta \end{pmatrix}, \tag{5}$$

where $s_\eta = \sin\eta$, $c_\xi = \cos\xi$ and so on.

On the earth, the experiment is located at a point of latitude δ. The local coordinate system (x, y, z) is defined such that the z-axis is in the direction of the e^- beam which is in a horizontal plane with respect to the surface of the earth, the y-axis is vertical and the x-axis is perpendicular to the y-z plane. This is, to a good approximation, the same definition as used in the OPAL experiment[1]. The angle between the z-axis and the direction of north is denoted by α (measured counter-clockwise, see Figure 1). As the earth rotates, the local coordinate system moves around the Z-axis. The time-dependent azimuthal angle, $\zeta(t)$, of the location of the experiment with respect to the X-axis is given by,

$$\zeta = \omega t, \tag{6}$$

where $\omega = 2\pi/T_{sd}$ with sidereal day T_{sd}, the time taken for one complete rotation of the earth around its axis.

Elements of the vector $\mathbf{c}_E$ in the local coordinate system (x, y, z) are obtained by successive rotations of the coordinate axes [6]:

$$\mathbf{c}_E = R \cdot \mathbf{c}_E^0 \tag{7}$$

$$R = R_y(\alpha) R_z(-\pi/2) R_y(-\delta) R_z(\zeta) \tag{8}$$

yielding

$$\mathbf{c}_E = \begin{pmatrix} s_\alpha s_\delta \\ c_\delta \\ -c_\alpha s_\delta \end{pmatrix} s_\eta \cdot \cos(\zeta - \xi) + \begin{pmatrix} c_\alpha \\ 0 \\ s_\alpha \end{pmatrix} s_\eta \cdot \sin(\zeta - \xi) + \begin{pmatrix} -s_\alpha c_\delta \\ s_\delta \\ c_\alpha c_\delta \end{pmatrix} c_\eta. \tag{9}$$

The elements in the brackets form three constant vectors which are determined by the location of the accelerator and orientation of the e^- beam at the experiment. The coefficients of these three constant vectors depend on the unique direction in the primary frame (η and ξ) and the phase of the earth's rotation ζ. There are two distinct components, one which varies with time and one which is constant. When the angle $\eta = 0$, i.e. the vector $\mathbf{c}_E$ is parallel to the rotation axis of the earth, the time-dependent component vanishes. The ϕ dependence of Δ_{NC} (Equation 3) in general exists, but vanishes in the special configuration where $\eta = 0$ and the experiment is located on the equator with e^- beam pointing to the north ($\alpha = 0$, $\delta = 0$) or south. The OPAL experiment is located at the latitude $\delta = 46.29°$ N and the longitude of $6.11°$ E with the angle $\alpha = 33.69°$ [13].

In this analysis, we choose the X-axis to point in the direction of the vernal equinox in the Pisces constellation. Due to the precession of the earth, and other reasons, the direction of the vernal equinox

[1] The LEP ring is not precisely horizontal but it is tilted by $0.8°$. However, for the purposes of this analysis this angle is small and will thus be neglected.

varies with time over a period of many years. However, for the limited duration of LEP operation, its motion can be neglected. In this approximation, the angle ζ at time t is given by

$$\zeta = \frac{2\pi}{T_{sd}}(t - t_0) + \zeta_0 \tag{10}$$

where T_{sd} is the average sidereal day (23h 56min 4.09053sec) [14], and ζ_0 is the azimuthal angle of the LEP location at time t_0, chosen to be the moment of vernal equinox in 1995: t_0 = 21st March 1995, 02h 14min (UT) [15]. The angle ζ_0 at that time is $\zeta_0 = 219.6^\circ$. Each OPAL event has a time stamp, so the angle ζ can be determined for each event.

In summary, for the OPAL experiment,

$$\alpha = 33.69^\circ \quad ; \quad \delta = 46.29^\circ \quad ; \quad \zeta = \frac{2\pi}{T_{sd}}(t - t_0) + \zeta_0 \tag{11}$$

while the direction of the $\mathbf{c}_E$ vector (η and ξ) and the energy scale $\Lambda_{\rm NC}$ are unknown.

4 Data analysis

To search for the effects of NCQED we use events selected as $e^+e^- \to \gamma\gamma(\gamma)$ as described in detail in [16]. The events were collected from a data sample corresponding to an integrated luminosity of 672.3 pb^{-1} taken at the highest LEP centre-of-mass energies, between 181 GeV and 209 GeV, during the last four years of OPAL operation. The luminosity-weighted mean centre-of-mass energy is 196.6 GeV. In total, 5235 events with at least two photons observed in the region $|\cos\theta_\gamma| < 0.93$ are selected, where θ_γ is the photon angle. No restrictions on either the angle between the two highest-energy photons or the number of additional photons are applied. The estimated background is less than 0.3%. The excellent uniformity and hermeticity of the OPAL detector provide a high and uniform efficiency of 98% over the entire range of azimuthal angle ϕ and for $|\cos\theta_\gamma| < 0.80$. Only in the range $0.80 < |\cos\theta_\gamma| < 0.93$ do larger corrections have to be applied. The experimental systematic uncertainties are small, typically 0.8%. The error on the theoretical prediction of the Standard Model QED is assumed to be 1%. This theoretical error arises from the correction of the observed angular distribution to the Born level at which the model predictions and measured cross-sections are given. This correction involves the angular definition of events with a topology other than two back-to-back photons. As in [16] the event polar angle convention chosen is $\cos\theta = \left|\sin\frac{\theta_1-\theta_2}{2}\right| \,/\, \left(\sin\frac{\theta_1+\theta_2}{2}\right)$, where θ_1 and θ_2 are the polar angles of the two highest-energy photons. The event azimuthal angle ϕ is chosen to be the azimuthal angle of the photon with largest $\cos\theta_\gamma$ out of the two highest-energy photons.

In NCQED the differential cross-section depends on three kinematic variables: the polar angle θ, the azimuthal angle ϕ, and the time via the orientation angle ζ. For each of these three variables, a fit to the model prediction is performed with the cross-section integrated (or averaged) over the other two. For example, the θ dependence is studied with a distribution integrated over ϕ and averaged over ζ. Similarly, the total cross-section, integrated over θ and ϕ, is analysed as a function of ζ. Because the region of large $\cos\theta$ is dominated by the Standard Model, the relative effects of NCQED are enhanced by restricting the θ integration to $\cos\theta < 0.6$, leading to a subsample of 1800 events.

The luminosity delivered by LEP is not uniformly distributed over time. On average more data were collected at night than during the day, leading to a dependence of the luminosity on ζ with a variation of 13%. This effect is taken into account in the determination of the cross-sections. The total integrated

luminosity is determined using small-angle Bhabha scattering in the region 25 mrad $< \theta <$ 59 mrad. The ζ dependence of the luminosity is obtained from the rate of Bhabha events detected in the electromagnetic calorimeter ($|\cos\theta| < 0.96$) in the same data sample as used for the analysis. Here we assume that any NCQED effects on Bhabha scattering can be neglected since the cross-section is dominated by forward scattered events for which the effects of NCQED are expected to be small [5].

To obtain a log likelihood curve which is approximately parabolic a fit parameter ε is chosen such that $\Lambda_{\rm NC} = (|\varepsilon|)^{-1/4}$. The non-physical region of negative ε is included in the fit by replacing $\sin^2\Delta_{\rm NC}$ by $-\sin^2\Delta_{\rm NC}$ in Equation 2 if ε is negative. Integration and averaging of this cross-section is done numerically.

4.1 The $\cos\theta$ distribution

Although the NCQED contribution $\Delta_{\rm NC}$ depends on several unknown model parameters ($\Lambda_{\rm NC}$, η, ξ), the dependence on η and ξ is greatly reduced when the cross-section is integrated over ϕ and averaged over time (i.e. $\zeta - \xi$). In this case, the only relevant kinematic variable in the differential cross-section is the production polar angle θ, and deviations from QED depend mainly on the unknown parameter $\Lambda_{\rm NC}$. For the orientation of OPAL the dependence on the parameter η is very weak. The effects are largest at $\cos\theta = 0$, here the variation of the cross-section with η is $\sim 0.2\%$. Therefore the result obtained on $\Lambda_{\rm NC}$ from the $\cos\theta$ distribution is almost independent of η. However, this decoupling is accidental; for other values of α the $\cos\theta$ distribution might vary by up to 40% relative to the average as a function of η.

The measured $\cos\theta$ distribution, at the luminosity-weighted average centre-of-mass energy, is shown in Figure 2. This distribution is sensitive to the parameter $\Lambda_{\rm NC}$. Since no significant deviation from QED is observed a limit on $\Lambda_{\rm NC}$ is set, assuming $\eta = 90^\circ$. This yields the most conservative result, since for this value of η the difference between QED and NCQED for a given $\Lambda_{\rm NC}$ is smallest. To obtain this limit, a simultaneous binned log-likelihood fit is performed to the differential cross-section distributions measured at eight centre-of-mass energy points and including systematic uncertainties and their correlations in the manner described in [16]. The result of this fit is given in Table 1. The corresponding one-sided limit at 95% confidence level of $\Lambda_{\rm NC} > 141$ GeV shown in Figure 3 as the dark grey region is valid for all η and, obviously, for all ξ.

4.2 The ϕ distribution

As discussed above, a ϕ-dependent cross-section is a characteristic signature of NCQED. The ϕ-dependence arises from the x and y components (c_{01}, c_{02}) of the vector $\mathbf{c}_E$. Since these components have a time-independent component (Equation 9), some ϕ-dependence remains even if the data are averaged over all ζ. However, for certain values of η, depending on the orientation of the experiment, the ϕ-dependence is washed out completely. In the configuration of the OPAL experiment at LEP, such a cancellation occurs for $\eta \approx 55^\circ$ (or 125°) as can be seen in Figure 4.

Figure 4 shows the measured ϕ distribution, at the luminosity-weighted average centre-of-mass energy, for $\mathrm{e^+e^-} \to \gamma\gamma$ integrated over $\cos\theta < 0.6$ and averaged over time. From this distribution 95% confidence level lower limits on $\Lambda_{\rm NC}$ are obtained as a function of η and independent of ξ. Table 1 summarises the fit results four four values of η. For $\eta = 90^\circ$ the best fit is two standard deviations away from the Standard Model. The result of that fit with a central value of $\Lambda_{\rm NC} = 1866^{-1/4}$ TeV = 152 GeV, as well as the limit for $\eta = 0^\circ$ are shown in Figure 4. For illustration the ϕ independent

Fit	Fit result [TeV^{-4}]	95% CL Limit [GeV]
$\cos\theta$ distribution		
$\eta = 90^\circ$	947^{+920}_{-905}	141
ϕ distribution		
$\eta = 0^\circ$	-174^{+703}_{-732}	167
$\eta = 30^\circ$	225^{+836}_{-841}	154
$\eta = 60^\circ$	1589^{+999}_{-982}	132
$\eta = 90^\circ$	1866^{+913}_{-900}	131

Table 1: Results of the fits to the $\cos\theta$ distribution and the ϕ distribution at several values of η. The fit result is given for the fit parameter ε. For $\Lambda_{\rm NC}$ the one-sided limit at 95% confidence level is given.

expectation at $\eta = 55^\circ$ at a low scale of $\Lambda_{\rm NC} = 120$ GeV is added to the plot. Limits for all values of η are shown in Figure 3 as the light grey region. The limit is strongest for $\eta = 0^\circ$ and weakest for $\eta = 73^\circ$. For some values of η the modulation in ϕ is small and sensitivity is lost due to the integration over $\cos\theta$, leading to a large uncertainty on ε. A better strategy would be a two-dimensional fit to $\mathrm{d}^2\sigma/\mathrm{d}\cos\theta\mathrm{d}\phi$. This analysis could be performed in several bins of ζ to avoid the loss of information due to the integration over time. However, such an analysis is not feasible given the available data statistics.

4.3 The total cross-section

The limits given above are obtaind from time-averaged distributions and hence give no information about the third model parameter ξ. This information could be provided by the total cross-section which depends on $\zeta - \xi$. However, any limit on $\Lambda_{\rm NC}$ determined from the total cross-section in dependence of ξ would be weaker than the limits given above, since the differential cross-sections in $\cos\theta$ or ϕ provide the strongest sensitivity to the scale $\Lambda_{\rm NC}$. But if a signal were observed, the unique time structure of the total cross-section would allow the determination of the angle ξ.

Figure 5 shows the total cross-section, at the luminosity-weighted centre-of-mass energy, integrated over θ and ϕ, as a function of the time-dependent angle ζ. The distribution has a $\chi^2/\mathrm{dof} = 39.9/30$ with respect to the Standard Model expectation which corresponds to a probability of 11%. Since no signal is observed in either the $\cos\theta$ or the ϕ distribution, no attempt is made to extract ξ from a fit to the measured total cross-section. However, examples of two model expectations are shown in Figure 5 together with the time independent case of $\eta = 0^\circ$.

5 Conclusion

Non-commutative QED would lead to deviations from the Standard Model depending on some energy scale $\Lambda_{\rm NC}$ and on a unique direction in space given by the angles η and ξ. The experimental signature of such a theory for the process $\mathrm{e^+e^-} \to \gamma\gamma$ was evaluated for the orientation of the OPAL detector and compared to the measurements. No significant deviations from the Standard Model predictions were observed. Distributions of the scattering angle θ were used to extract a lower limit on the energy

scale $\Lambda_{\rm NC}$ of 141 GeV at the 95% confidence level, which is valid for all angles η and ξ. Using the ϕ distributions this limit was improved for some values of η up to $\Lambda_{\rm NC} > 167$ GeV. The total cross-section gives weaker limits but its time dependence could in principle be used to determine the third model parameter ξ if a signal were observed. These are the first limits obtained on NCQED from an e^+e^- collider experiment.

Acknowledgements

We would like to thank J. Kamoshita and K. Hagiwara for useful discussions.
We particularly wish to thank the SL Division for the efficient operation of the LEP accelerator at all energies and for their close cooperation with our experimental group. In addition to the support staff at our own institutions we are pleased to acknowledge the
Department of Energy, USA,
National Science Foundation, USA,
Particle Physics and Astronomy Research Council, UK,
Natural Sciences and Engineering Research Council, Canada,
Israel Science Foundation, administered by the Israel Academy of Science and Humanities,
Benoziyo Center for High Energy Physics,
Japanese Ministry of Education, Culture, Sports, Science and Technology (MEXT) and a grant under the MEXT International Science Research Program,
Japanese Society for the Promotion of Science (JSPS),
German Israeli Bi-national Science Foundation (GIF),
Bundesministerium für Bildung und Forschung, Germany,
National Research Council of Canada,
Hungarian Foundation for Scientific Research, OTKA T-029328, and T-038240,
The NWO/NATO Fund for Scientific Reasearch, the Netherlands.

References

[1] H.S. Snyder, Phys. Rev. **71** (1947) 38, Phys. Rev. **72** (1947) 68.

[2] A. Connes, M.R. Douglas and A. Schwarz, J. High Energy Phys. **02** (1998) 0003;
N. Seiberg and E. Witten, J. High Energy Phys. **09** (1999) 032.

[3] I. Hinchliffe and N. Kersting, "Review of the Phenomenology of Noncommutative Geometry", hep-ph/0205040.

[4] M. Dubois-Violette, R. Kerner and J. Madore, J. Math. Phys. **39** (1998) 730;
S. Doplicher, K. Fredenhagen and J.E. Roberts, Commun. Math. Phys. **172** (1995) 187.

[5] J.L. Hewett, F.J. Petriello and T.G. Rizzo, Phys. Rev. **D64** (2001) 075012;
J.L. Hewett private communication: expressions for Δ_{PA} have a missing factor of 2.

[6] J. Kamoshita, "Probing Noncommutative Space-Time in the Laboratory Frame", hep-ph/0206223.

[7] M. Hayakawa, Phys. Lett. **B478** (2000) 394.

[8] P. Mathews, Phys. Rev. **D63** (2001) 075007.

[9] M. Chaichian, M. M. Sheikh-Jabbari and A. Tureanu, Phys. Rev. Lett. **86** (2001) 2716.

[10] H. Falomir *et al.*, Phys. Rev. **D66** (2002) 045018.

[11] S. M. Carroll *et al.*, Phys. Rev. Lett. **87** (2001) 141601.

[12] L. A. Page, Phys. Rev. **106** (1957) 394.

[13] M. Jones, "Computation of geodetic coordinates and azimuths at the LEP interaction points", EDMS document 322742v.1 (1999), `http://edms.cern.ch/file/322742/1/geod_param_lep_ip.pdf`.

[14] D.E. Groom *et al.*, Eur. Phys. J. **C15** (2000) 74.

[15] `http://aa.usno.navy.mil/data/docs/EarthSeasons.html`.

[16] OPAL Collaboration, G. Abbiendi *et al.*, Eur. Phys. J. **C26** (2003) 331.

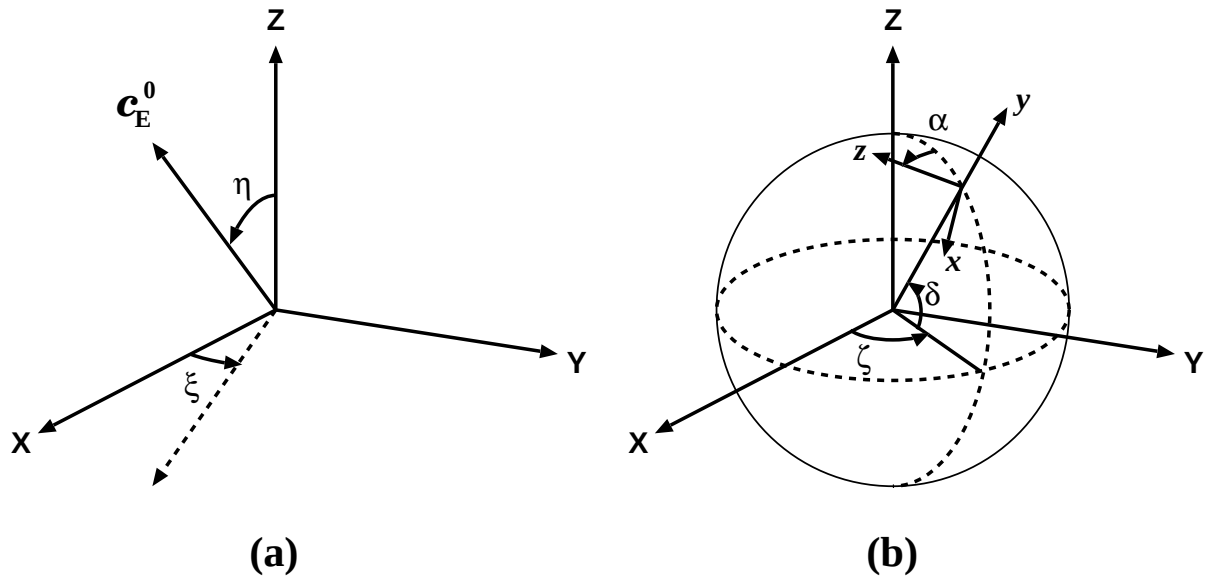

Figure 1: Definition of the two coordinate systems: (a) the primary frame (X, Y, Z) in which the vector $\mathbf{c}_E^0$ is fixed, and (b) the local coordinate system (x, y, z) of an e^+e^- experiment on the earth.

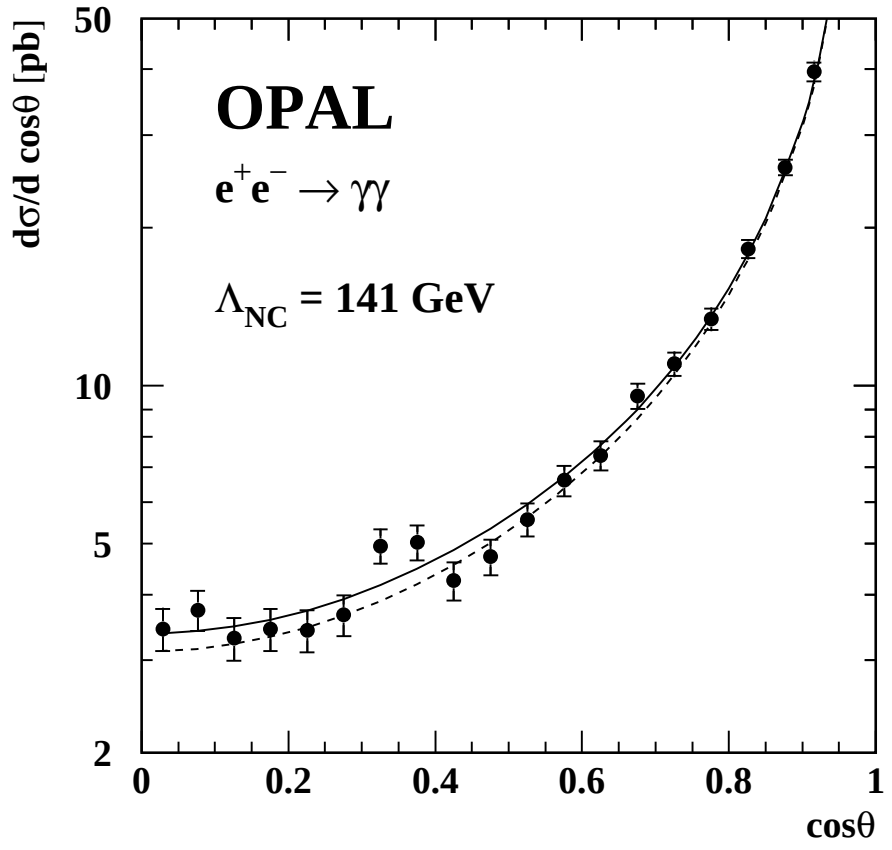

Figure 2: The measured differential cross-section as a function of $\cos\theta$. The points are OPAL data, the solid line shows the Standard Model prediction and the dashed line corresponds to the 95% confidence level limit of $\Lambda_{\rm NC} = 141$ GeV and $\eta = 90°$.

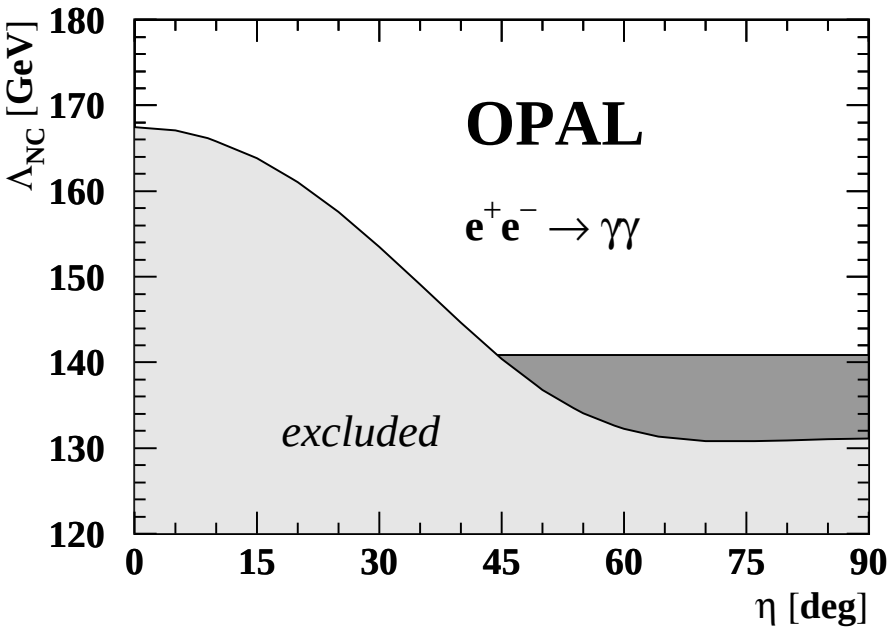

Figure 3: One-sided 95% confidence level limits on the energy scale $\Lambda_{\rm NC}$ as a function of the angle η. The light grey region is derived from the observed ϕ distribution and the η-independent limit shown in dark grey results from the observed $\cos\theta$ distribution.

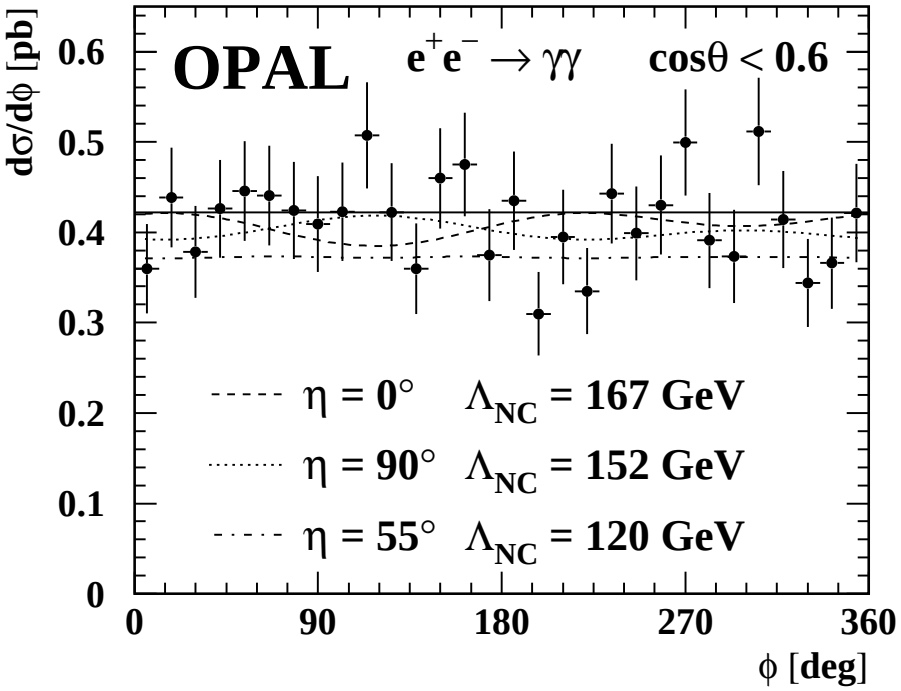

Figure 4: Measured ϕ distribution. The points are OPAL data and the solid line the Standard Model prediction. Expectations from NCQED are shown for the best limit of $\Lambda_{\rm NC} > 167$ GeV at $\eta = 0°$ and the best fit at $\eta = 90°$ which yields $\Lambda_{\rm NC} = 152$ GeV. The ϕ independent distribution at $\eta = 55°$ is shown as well.

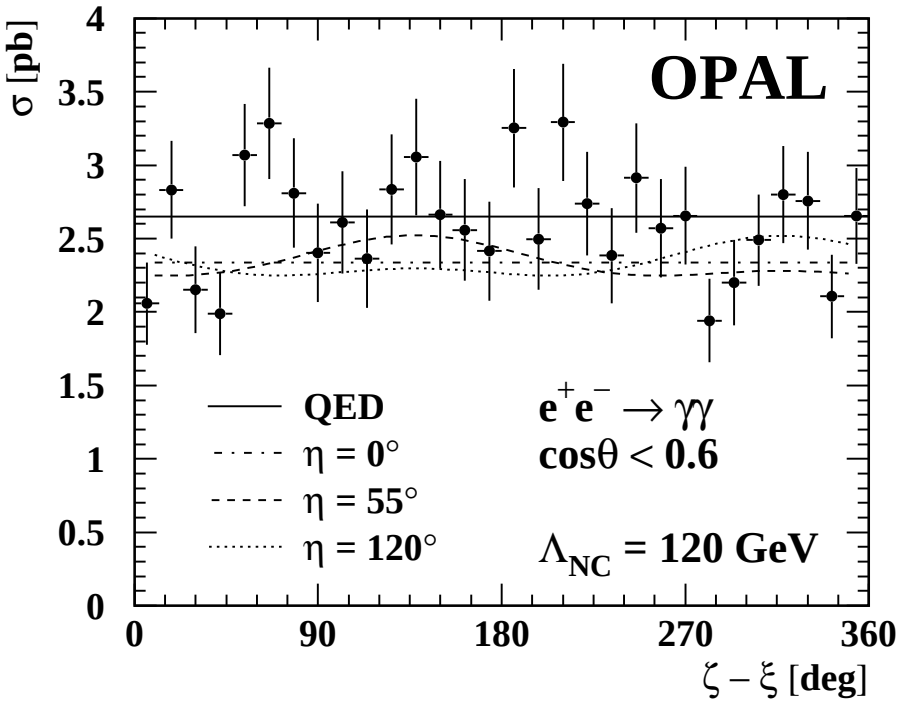

Figure 5: Total cross-section as a function of the time-dependent $\zeta - \xi$. The points are OPAL data and the solid line represents the Standard Model prediction. To guide the interpretation of the data the expectations from NCQED are shown for a low scale of $\Lambda_{\rm NC} = 120$ GeV. Three values of η (0°, 55°, 120°) are shown.